JGR Oceans

RESEARCH ARTICLE
10.1029/2020JC016102

Interaction Between Mesoscale Eddies and the Gyre Circulation in the Lofoten Basin

R. P. Raj[1,2], I. Halo[3,4,5], S. Chatterjee[6], T. Belonenko[7], M. Bakhoday-Paskyabi[8,2], I. Bashmachnikov[7,9], A. Fedorov[7,9], and J. Xie[1]

[1]Nansen Environmental and Remote Sensing Center, Bergen, Norway, [2]Bjerknes Centre for Climate Research, Bergen, Norway, [3]Conservation and Marine Sciences, Cape Peninsula University of Technology, Cape Town, South Africa, [4]Centre for Sustainable Oceans, Cape Peninsula University of Technology, Cape Town, South Africa, [5]Nansen-Tutu Center for Marine Environmental Research, University of Cape Town, Cape Town, South Africa, [6]National Centre for Polar and Ocean Research, Ministry of Earth Sciences, Vasco da Gama, India, [7]Department of Oceanography, Saint Petersburg State University, Saint Petersburg, Russia, [8]Geophysical Institute and Bergen Offshore Wind Centre, University of Bergen, Bergen, Norway, [9]Nansen International Environmental and Remote Sensing Centre, Saint-Petersburg, Russia

Abstract The interaction between the mesoscale eddies and the cyclonic gyre circulation of the Lofoten Basin is studied using a suite of satellite altimeters, a regional coupled ocean-sea-ice data assimilation system (the TOPAZ reanalysis) and Argo float data. An automated method identified 5,373/5,589 individual anticyclonic/cyclonic eddies in the Lofoten Basin from more than 65,000 altimeter-based eddy observations, of which 70–85% are found to be nonlinear. The nonlinearity of eddies is estimated from its translational and rotational velocities. The study found clustering of highly intense nonlinear eddies on either side of the Lofoten Basin. Further, we show the distinct cyclonic drift of the anticyclonic and cyclonic eddies, both confined to the western side of the basin, and its similarity to the middepth gyre circulation also confined to the same region. A well-defined cyclonic drift pattern of eddies is found during the time period when the gyre circulation of the basin is strengthened, while a clear cyclonic drift of eddies is absent during a weakened gyre. Analysis of barotropic energy conversion in the reanalysis data shows maximum transfer of energy from the eddy field to the mean flow in the Lofoten Vortex region. Even though comparatively smaller (roughly 9 times) there is also notable transfer of energy from the mean flow to the eddies in the region located outside the Lofoten Vortex. Our study shows that the gyre circulation when strengthened, receives more energy from the Lofoten Vortex and loses less energy to those eddies circulating around the Lofoten Vortex.

Plain Language Summary Lofoten Basin situated in the path of Atlantic Water flow from the North Atlantic to the Arctic is the largest heat reservoir in the Nordic Seas. The mesoscale eddies and the gyre circulation of the basin can impact the heat transported into the basin interior and the heat lost to the atmosphere. In this paper, we use a suite of satellite altimeters, Argo floats, and an ocean reanalysis data set to study the interaction between the mesoscale eddies and the gyre circulation of the Lofoten Basin. Our study shows that the energy transfer associated with the mesoscale eddies influence the gyre circulation of the basin.

Key Points:
- Cyclonic drift of mesoscale eddies in the western Lofoten Basin resembles the pattern of the cyclonic gyre circulation
- A well-defined cyclonic drift of eddies is found when the gyre circulation strengthens, while it is not present when the gyre weakens
- Energy exchange between eddies and the mean circulation of the Lofoten Basin influence the strength of the gyre

Supporting Information:
- Supporting Information S1

Correspondence to:
R. P. Raj,
roshin.raj@nersc.no

Citation:
Raj, R. P., Halo, I., Chatterjee, S., Belonenko, T., Bakhoday-Paskyabi, M., Bashmachnikov, I., et al. (2020). Interaction between mesoscale eddies and the gyre circulation in the Lofoten Basin. *Journal of Geophysical Research: Oceans*, *125*, e2020JC016102. https://doi.org/10.1029/2020JC016102

Received 20 JAN 2020
Accepted 1 JUN 2020
Accepted article online 4 JUN 2020

1. Introduction

The Lofoten Basin, the major heat reservoir of the Nordic Seas, is located in its eastern part along the advection path of Atlantic Water (AW) from the North Atlantic to the Arctic (Figure 1). The circulation of the basin has been a subject of investigation since the Norwegian North-Atlantic Expedition during 1876–1878 (Helland-Hansen & Nansen, 1909; Mohn, 1887). The two branches of the Norwegian Atlantic Current, the Norwegian Atlantic Front Current and the Norwegian Atlantic Slope Current (hereafter termed as the slope current) border the western and eastern part of the basin (Orvik & Niiler, 2002; Orvik & Skagseth, 2003; Skagseth & Orvik, 2002). Poulain et al. (1996), Orvik and Niiler (2002), and Jakobsen et al. (2003) were among the first to observe the cyclonic gyre circulation of the Lofoten Basin which is strongly linked to the topography and driven mainly by winds. These studies using surface drifters confirm the link between the surface circulation and bottom topography noted many decades before by

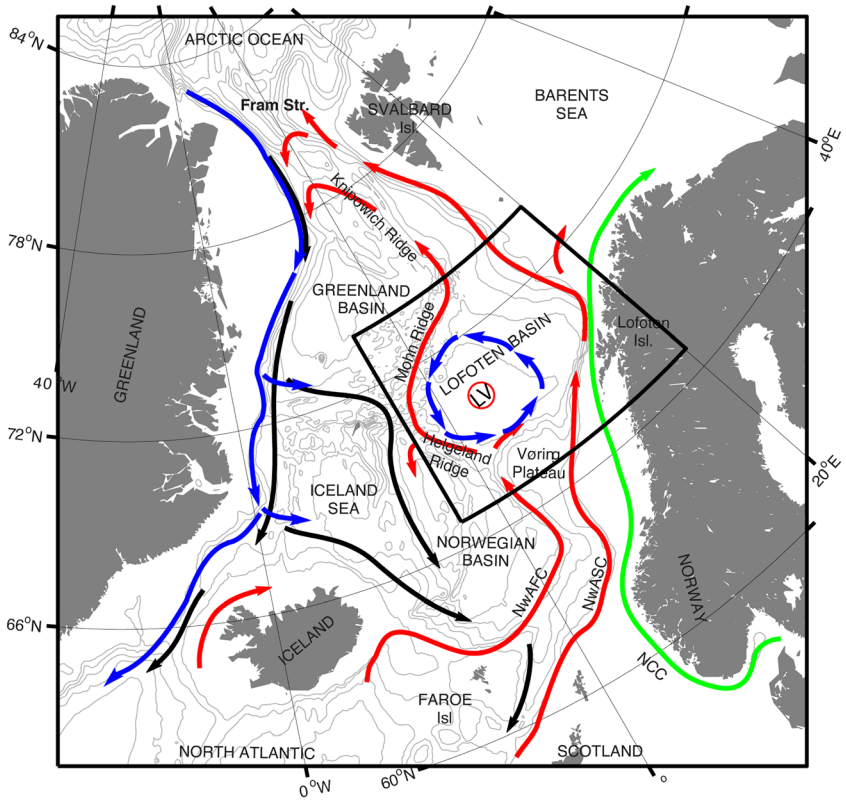

Figure 1. The Nordic Seas with schematic pathways indicating the overturning circulation from warm inflowing Atlantic water in the surface (red) to cold and dense overflows to the deep North Atlantic (black). The Norwegian Atlantic slope current (NwASC), here termed as the slope current and the Norwegian Atlantic front current (NwAFC) are represented by red arrows. The fresh Norwegian coastal current (NCC) and the East Greenland current are indicated, respectively, in green and blue. The cyclonic gyre circulation in the Lofoten Basin is marked by blue arrows. The location of the Lofoten vortex (LV; red circle) in the western Lofoten Basin is also indicated in the figure. Gray isobaths are drawn for every 600 m.

Helland-Hansen and Nansen (1909). Isachsen et al. (2003) later confirmed that on monthly to annual time scales the wind forcing is more important than hydrographic (thermal wind shear) forcing for the gyre flow along f/H-contours (f, Coriolis parameter; H, ocean depth). Nearly a decade later, Voet et al. (2010) performed a comprehensive observation-based (Argo floats) study of the mean circulation at mid-ocean depths (1,000 m) of the Lofoten Basin and showed that the cyclonic middepth circulation is strongly coupled with the structure of the bottom topography. Furthermore, their study confirms the model results of Nøst and Isachsen et al. (2003) which showed that within closed f/H contours the bottom velocity is dependent on the local slope of the f/H field and on the integrated forcing within that contour. Interestingly, Voet et al. (2010) also found that the seasonality of the Lofoten Basin gyre circulation cannot be fully explained by the wind forcing alone and hypothesized that mesoscale eddies in the basin may have a significant impact on the gyre.

Focusing on the mesoscale variability, it is well-documented that the Lofoten Basin is the most eddy active region in the Nordic Seas (Jakobsen et al., 2003; Poulain et al., 1996; Raj et al., 2015, 2016; Volkov et al., 2013; Zinchenko et al., 2019). An important feature of the mesoscale circulation of the basin is the detachment of eddies from the slope current and its southwestward propagation, which in turn transports the warm and saltier AW into the basin interior (Andersson et al., 2011; Rossby et al., 2009). AW thus transported occupies the basin down to a depth of roughly 800 m, the result of which the Lofoten Basin is the largest heat reservoir in the Nordic Seas (Blindheim & Rey, 2004). This lateral transport of AW heat via the eddies also mediates the gradual cooling of the slope current on its way toward the Arctic (Isachsen et al., 2012).

The Lofoten Basin also hosts a quasi-permanent anticyclonic eddy, the Lofoten Vortex, at its deepest part (e.g., Köhl, 2007; Raj et al., 2015). The vortex is sustained by receiving energy from other anticyclonic

eddies in the Lofoten Basin via eddy mergers (Köhl, 2007; Raj et al., 2015; Volkov et al., 2015). Deep winter convection is also a necessary condition for the quasi-permanent existence of this unique natural phenomenon as it creates a favorable setting for annual regeneration of the Lofoten Vortex (Bashmachnikov et al., 2017; Bloshkina & Ivanov, 2016; Fedorov et al., 2019; Travkin & Belonenko, 2019; Yu et al., 2017).

While eddies transport AW into the Lofoten Basin's interior, the gyre circulation in the basin has the important effect of storing this large quantity of AW within the basin (Belonenko et al., 2014; Gascard & Mork, 2008; Orvik, 2004; Volkov et al., 2013). As a result, the residence time of AW in the Lofoten Basin is larger than in any other region in the Nordic Seas. The longer residence time of AW combined with strong atmospheric cooling results in excessive loss of AW heat in the basin. In concurrence, the Lofoten Basin is categorized as a region with large heat loss in the Nordic Seas (Segtnan et al., 2011). Furthermore, it is also the location where the bulk of light to dense water mass transformation in the entire Nordic Seas takes place (Isachsen et al., 2007; Segtnan et al., 2011). The excess heat loss in the Lofoten Basin is important since anomalous heat transported downstream of the basin is known to influence the sea ice cover in the Barents Sea (Årthun et al., 2012; Sandø et al., 2010), and the regional climate of Svalbard (Walczowski & Piechura, 2011). Hence, it can be argued that the mesoscale eddies and the gyre circulation of the Lofoten Basin are of high importance for the oceanic and the sea ice conditions in the Nordic Seas.

The mesoscale eddies and the cyclonic gyre circulation in the Lofoten Basin have been extensively studied, but separately (described above). Nevertheless, there has been few studies that hypothesized the interaction between the two. For example, Voet et al. (2010) hypothesized that the mesoscale eddies of the Lofoten Basin may impact the gyre circulation of the basin, while Raj et al. (2015) suggested that the Lofoten Basin gyre circulation is likely to assist the drift of anticyclonic eddies (AEs) spun from the slope current into the western Lofoten Basin where they merge with the Lofoten Vortex. Apart from this, a dedicated effort focusing on the interaction between the two is missing. In this study, we use a suite of satellite altimeter, Argo floats, and ocean reanalysis data set to study the interaction between the mesoscale eddies and the gyre circulation in the Lofoten Basin.

2. Data and Methods

2.1. Satellite Altimetry

Monitoring of mesoscale eddies in the Lofoten Basin has been facilitated by the launch of multisatellite altimeter missions combined with the implementation of better interpolation methods in satellite altimeter data processing. High-resolution sea level anomalies (SLA) for nearly two and a half decades (January 1993 to December 2018) are used in this study. These gridded SLA data (SEALEVEL_GLO_PHY_L4_REP_OBSERVATIONS_088_047), obtained from Copernicus Marine Environment Monitoring Services (CMEMS, http://marine.copernicus.eu/), have been completely reprocessed to exploit the most recent advances in each of the successive processing steps and to provide a product of homogeneous quality (Capet et al., 2014). The new reprocessing includes important modifications of the processing chain (a new reference field, revised intercalibration, a new ocean tidal component, new sensor-specific instrumental, and atmospheric corrections) adopted to convert raw altimeter sensor signals to along-track and, finally, gridded sea level data. The SLA fields (0.25° regular Cartesian) are based on merged TOPEX, JASON 1, 2, ERS-1, 2, GFO, CryoSat-2, HY-2A, SARAL/AltiKa, and Envisat data. Even though the latitudinal coverage of the TOPEX/Poseidon and Jason altimeters is 66°N, these measurements are used as a reference to remove long-wavelength error (e.g., orbit error, altimeter biases) in other satellite missions (Le Traon & Ogor, 1998).

2.1.1. Identification of Mesoscale Eddies

Several eddy detection schemes are available for the automated detection of eddies (Raj & Halo, 2016). The most commonly used methods are based on the geometric criteria (Chelton et al., 2011), dynamical criteria (Isern-Fontanet et al., 2006) and the hybrid method, which combined the use of geometric as well as the dynamical criteria (Raj et al., 2016). In order to identify eddies in the Lofoten Basin, we use an automatic hybrid eddy detection algorithm that has been used successfully in several oceanic basins (Halo, 2012; Halo et al., 2014), especially in the Lofoten Basin (Raj et al., 2015, 2016; Raj & Halo, 2016). To avoid the influence of the land contamination on altimeter data, the detection of eddies is limited to 30 km offshore of the Lofoten coast. The hybrid algorithm uses simultaneously geometric and dynamical properties of the flow

field to identify an eddy and is likely to be better than using a single criterion. The geometric component regards the closed near-circular contour of SLA, whereas the dynamical property regards the instantaneous field within the closed contour where the vorticity field dominates the strain rate or deformed flow field following the Okubo-Weiss formulation (Chelton et al., 2007; Isern-Fontanet et al., 2006): $W = (S_s^2 + S_n^2) - \varsigma^2$, where "W" denotes the Okubo-Weiss parameter, vorticity is defined as $\varsigma = \frac{\partial v'}{\partial x} - \frac{\partial u'}{\partial y}$, and Strain ($S$) includes both shear ($S_s$) and normal ($S_n$) components, $S^2 = S_s^2 + S_n^2$. $S_s = \frac{\partial v'}{\partial x} + \frac{\partial u'}{\partial y}$, $S_n = \frac{\partial u'}{\partial x} - \frac{\partial v'}{\partial y}$, where u' and v' represent the horizontal components of geostrophic velocity anomalies in x and y directions estimated from the SLA using the classic geostrophic relation (e.g., Raj et al., 2016). Negative W implies domination of vorticity over strain, an essential feature of eddies. Note that in contrast with Chelton et al. (2011), no threshold value is imposed on W to minimize subjectivity, and the contours intervals are set to the precision of altimetric observation which is 2 cm. More details of the algorithm are presented in Halo (2012).

The tracking of eddies in space and consecutive time steps is done with reference to the centers of each eddy observation, in a generalized nondimensional property space, following the method proposed by Penven et al. (2005). More details of tracking of Lofoten Basin eddies from altimeter data are presented in Raj et al. (2015, 2016) and Raj and Halo (2016). A limitation of the eddy tracking method used here is the premature termination of eddy tracks due to an absence of surface eddy signatures for a short period, which can influence the estimation of eddy life. An alternative is used to use a fake eddy during its absence (Faghmous et al., 2015), or similar to the one used in the AVISO eddy data set (Duacs/Aviso+, 2019), where the tracking procedure allows the loss of one to three consecutive observations.

The radius of the eddies are estimated from their respective surface area (A), and eddy kinetic energy is estimated as: $EKE = \frac{u'^2 + v'^2}{2}$, while eddy intensity is defined as the area weighted mean EKE over the eddy area: $EI = \frac{1}{A}\int_A EKE \, dA$, following Raj et al. (2015). The statistical significance (at the 95% confidence level) of the difference in the mean EI of eddies is computed by using the two-sample t test for equal means (Snedecor & Cochran, 1989).

2.2. TOPAZ Reanalysis Data

TOPAZ, which represents the Arctic Marine Forecasting Center of CMEMS, is a coupled ocean and sea ice data assimilation system for the North Atlantic and the Arctic that is based on the Hybrid Coordinate Ocean Model (HYCOM) and the Ensemble Kalman Filter data assimilation (Xie et al., 2017). TOPAZ results used here for the time period 1993–2018, have been validated in several studies (Chatterjee et al., 2018; Lien et al., 2016; Raj et al., 2019; Xie et al., 2017). HYCOM, the ocean model in TOPAZ, has 28 hybrid z-isopycnal layers at a horizontal resolution of 12 to 16 km in the Nordic Seas and the Arctic. TOPAZ, forced by the ECMWF ERA Interim reanalysis, assimilates almost all available measurements including along-track altimetry data, sea surface temperature, sea ice concentration, and sea ice drift from satellites along with in situ temperature and salinity profiles. In TOPAZ, small mesoscale eddies and submesoscale eddies are parameterized. Note that the Lofoten Vortex is resolved in TOPAZ model results, an example is shown in Xie et al. (2020; see their Figure 41). The signature of cyclonic gyre circulation of the Lofoten Basin examined using TOPAZ data in section 3.4 can be seen in the surface layer of the TOPAZ data as well as deeper layers (e.g., 1,000-m depth; not shown).

Energy conversion rates in the eddy kinetic energy conservation equation is used to quantify the relative importance of instability and eddy-mean interaction mechanisms (e.g., Dong et al., 2007; Klein et al., 2008; Marchesiello et al., 2003). TOPAZ results are used for the computation of barotropic energy conversion terms (Halo et al., 2014; Marchesiello et al., 2003), derived from the volume-integrated evolution equation of the kinetic energy budget (Cronin & Watts, 1996; Fedorov & Belonenko, 2020; Kundu, 1990):

$$\mathrm{KmKe} = -\left[\overline{u'u'}\frac{\partial \overline{u}}{\partial x} + \overline{u'v'}\left(\frac{\partial \overline{u}}{\partial y} + \frac{\partial \overline{v}}{\partial x}\right) + \overline{v'v'}\frac{\partial \overline{v}}{\partial y}\right].$$

In here, $\overline{u}$ and $\overline{v}$ are the time-mean zonal and meridional components of velocities of the TOPAZ flow field, while u' and v' are the perturbations in time of the zonal and meridional components, and x, y are zonal and

meridional directions. If the conversion of mean kinetic energy to eddy kinetic energy KmKe (viz., barotropic conversion rate) is positive, it implicates the occurrence of shear instability in the extraction of kinetic energy from the mean flow to energize eddies.

2.3. Argo Floats

The hydrographic structure of mesoscale eddies of the Lofoten Basin is studied using delayed mode Argo profiling floats (ftp.ifremer.fr) for the time period August 1997 to December 2018. The data profiles have been quality controlled, and the adjusted salinity has been estimated by comparison with high-quality ship-based CTD data and the climatology (details given in http://www.argo.ucsd.edu/Argo_date_guide.html). The vertical profiles of AEs and cyclonic eddies (CEs) are obtained following the method proposed by Raj et al. (2016). The locations of the Argo floats are tested for colocation with corresponding altimeter-based daily latitude-longitude center positions and radii of AEs and CEs. After collocating in time, only those Argo floats that are inside half the radius of an altimeter-derived daily AE or CE are considered to be collocated with that eddy. Note that downward displacement of isotherms is typical at the center of anticyclonic eddies, while, on the other hand, the isotherms can be tilted upward in the periphery (e.g., Mizobata et al., 2002). Hence, by reducing the search area to half the eddy radius, the Argo floats residing in the peripheral region of eddies are avoided. This criterion is one of the best practical solutions to differentiate between the vertical structures of AEs and CEs using Argo float profiles (e.g., Raj et al., 2016).

3. Results and Discussions

During the past 26 years (1993–2018), our analysis identified around 11,000 individual mesoscale eddies (AEs: 5,373; CEs: 5,589) in the Lofoten Basin from more than 65,000 altimeter-based eddy observations. Validation of results obtained from the altimeter data using the hybrid eddy detection method is performed using Argo float profile data. It is well-known that the vertical structure of CEs and AEs is distinctly different. Therefore, it is expected that the AEs and CEs detected in our study will exhibit distinct vertical characteristics in order to infer that the altimeter data and the methodology used provide realistic signature of these mesoscale ocean features. Analysis (section 2.3) found 91 Argo float profiles collocated with the core of the AEs, while 74 inside the CEs (Figure 2a). The temperature and the density profiles of AEs and CEs show distinct signature where warm and less dense Atlantic Water has penetrated to deep ocean inside the AEs (Figures 2b and 2c).

The seasonality (winter, December–April; summer, May–September) in the vertical structure of the collocated Argo float profiles is also examined (Figure S1 in the supporting information). More Argo float profiles are collocated with eddies during summer (AEs, 42; CEs, 38) than during winter (AEs, 29; CEs, 27). While both types of eddies portray surface stratification during summer and mixing at the surface during winter, the difference is clearer at depths deeper below 200 m. All in all, Figures 2 and S1 show that the altimeter data and the hybrid eddy detection algorithm provide realistic results that can be further used to investigate the eddy activity of the basin.

3.1. Mesoscale Eddies or Rossby Waves?

As mentioned in section 1, the Lofoten Basin is well known as the most eddy active region in the entire Nordic Seas. However, it should be noted that a broad spectrum of mesoscale oceanic variability exists, hence waves and nonlinear eddies of different scales can cooccur (Wunsch, 2010) and indeed overlap (Tulloch et al., 2009). It is also a fact that mesoscale eddies often propagate with the phase speed of linear baroclinic Rossby waves (McWilliams & Flierl, 1979). In the Lofoten Basin, the existence of low-frequency waves has been reported earlier (Volkov et al., 2013). A time-averaged cyclonic wavelike propagation of the synoptic-scale SSH anomalies was revealed around the center of the Lofoten Basin in their study and is considered as barotropic topographic Rossby waves. These topographic waves formed due to the fact that topographic beta effect of the basin have a frequency range characteristic of Rossby waves. The phase speed of these waves (about 2 to 10 km/day) are also consistent with the drift speed of Lofoten Basin eddies (~5 km/day; Raj et al., 2016).

A way to differentiate nonlinear mesoscale eddies from nonlinear Rossby waves is by estimating the nonlinearity parameter of the detected eddies (Chelton et al., 2007, 2011). It is determined as the ratio of the rotation velocity "U" to the translation velocity "V_{drift}" of a mesoscale structure. U is defined as the maximum of

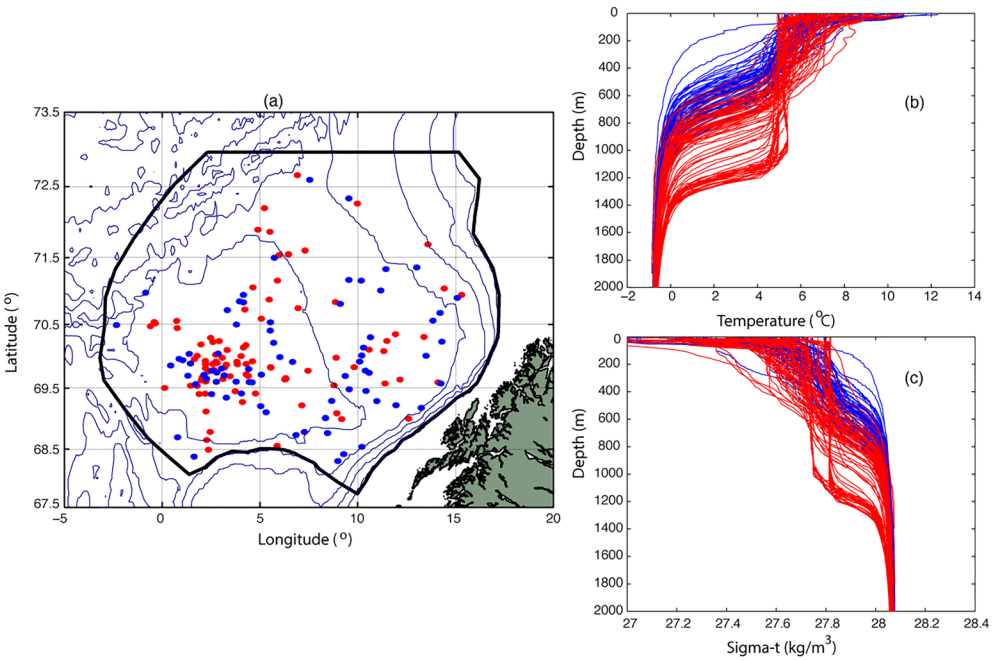

Figure 2. (a) Location of Argo floats identified within anticyclonic (red) and cyclonic (blue) eddies. The black polygon represents the Lofoten Basin region. Blue isobaths (ETOPO5 data) are drawn for every 500 m. (b) Temperature and (c) density profiles of Argo floats collocated within anticyclonic (red) and cyclonic (blue) eddies in the Lofoten Basin.

the average geostrophic speeds around all closed contours of SLA inside the eddy (Chelton et al., 2011). When the nonlinearity parameter exceeds one ($U/V_{\text{drift}} > 1$), it implies that the streamlines within the mesoscale structure are mostly closed and, thus, the structure represents a nonlinear eddy with a potential to trap material in their cores (Chelton et al., 2007, 2011; Early et al., 2011). The opposite (i.e., $U/V_{\text{drift}} < 1$) suggests the existence of open streamlines, which is typical for propagating waves (Early et al., 2011). Theiss (2004), while investigating a transition between waves and eddies, also computed an equivalent version of U/V_{drift} using the ratio of the Rhines scale ($L_R=\sqrt{U/\beta}$, where β is the variation of the Coriolis parameter with latitude) to the baroclinic Rossby radius of deformation (R_D), which shows the importance of the nonlinear terms relative to the β term in the quasi-geostrophic theory. For $L_R/R_D > 1$, the alternating zonal flows of Rossby waves become unstable and form nonlinear eddies.

Our analysis found that around 70–85% of the detected mesoscale structures satisfy the nonlinearity criteria (AEs: 84%; CEs: 70%). The 15–30% of the detected mesoscale structures, which do not satisfy the criteria, may represent topographic Rossby waves. Note that the smoothing associated with gridding of the altimeter data can result in reduction of the actual U, as well as errors in V_{drift}. Nevertheless, for the rest of the analyses we use only the mesoscale structures that satisfy the nonlinearity criteria. The respective mean radius, amplitude, EI, and drift speed are 37 km, 6.1 cm, 93 cm^2/s^2, and 7.2 km/day for the AEs, and 38 km, 5.6 cm, 76 cm^2/s^2, and 7.9 km/day for the CEs.

3.2. Surface Eddy Characteristics in the Lofoten Basin

The distribution of the number of eddy observations (Eobs) in the Lofoten Basin is bimodal (Figures 3a and 3b) with two distinct maxima on either side of the basin, as reported earlier (Raj et al., 2016; Raj & Halo, 2016). Similarly, the EI of both AEs and CEs also show distinct maximum on either side of the basin (Figures 3c and 3d). While higher number of Eobs and EI of AEs on the eastern part is associated with the eddies spun from the slope current, the same in the western Lofoten Basin is linked to the near permanent presence of the highly energetic Lofoten Vortex (Raj et al., 2015), which is partly maintained by the energy transfer during eddy mergers (Köhl, 2007; Travkin & Belonenko, 2019) and due to the formation of a homogeneous layer in the central part of the Lofoten Basin due to winter convection (e.g., Fedorov et al., 2019; Yu et al., 2017).

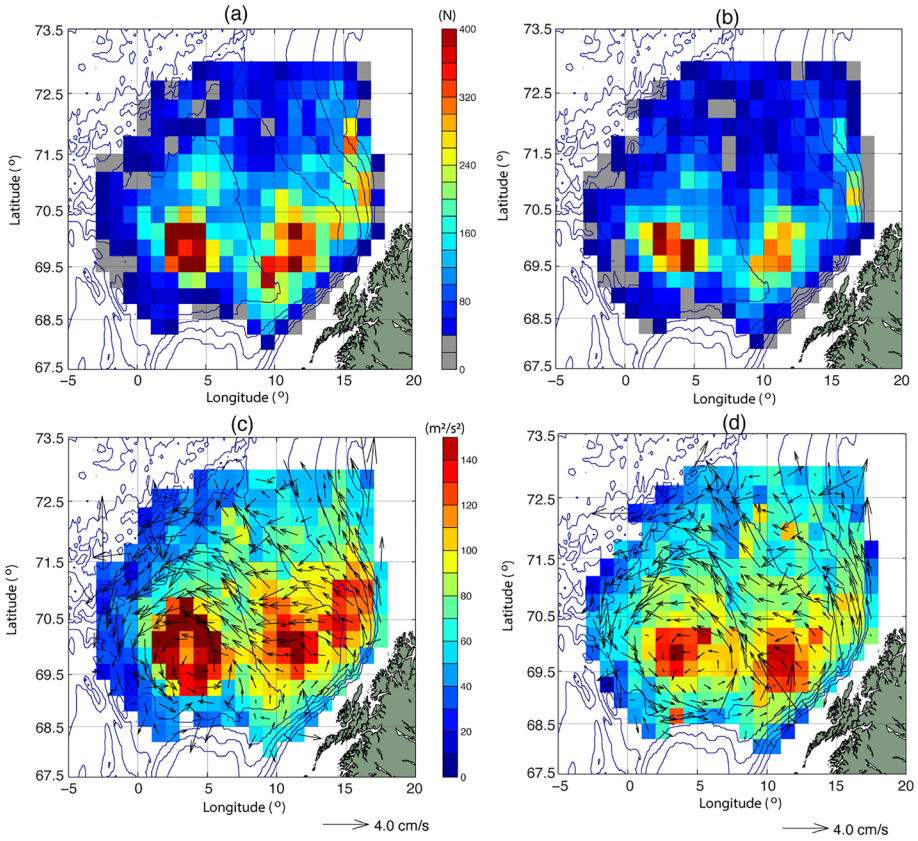

Figure 3. Total number of eddy occurrences of (a) anticyclonic and (b) cyclonic eddies in every 1° longitude and 0.3° latitude bins in the Lofoten Basin. Mean (bin average) EI (color) and drift velocity (vectors) of (c) anticyclonic and (d) cyclonic in the Lofoten Basin. Blue isobaths are drawn for every 500 m.

Focusing on the CEs (Figure 3d), the higher number of Eobs and EI in the eastern Lofoten Basin is linked to the eddy generation from the slope current, presumably due to baroclinic instability of the mean flow (Isachsen, 2015; Zinchenko et al., 2019). The interesting question of how CEs survive in the vicinity of the large Lofoten Vortex (Figure 3b), which in turn registers high EI in the western Lofoten Basin (Figure 3d) can be understood from the study of Dritschel (1989). They used a two-dimensional formulation to demonstrate that if large and small eddies of the same polarity coexist, the small eddy is pulled into the thread and wound on to the large vortex. On the contrary, small eddies of the opposite sign successfully resist the tensile effect of the flow of a large vortex and therefore survive as localized vortex formations near a large vortex. Thus, while AEs merge with the Lofoten Vortex, CEs persist. In turn, these CEs surrounding the Lofoten Vortex form a powerful ring of shielded vortices (Carton, 1992; Tóth & Házi, 2010) and can hinder the merging of AEs with the Lofoten Vortex, as has been shown by Köhl (2007) and Raj et al. (2015).

3.3. Eddy Drift and the Gyre Circulation

The drift of mesoscale eddies shown in Figures 3c and 3d reveals a distinct cyclonic circulation associated with both AEs and CEs, confined to the western side of the basin. The drift velocity is minimum at the deepest part of the basin. Other studies using altimeter data also found mesoscale eddies entering the western Lofoten Basin from the east to follow a cyclonic route (Raj & Halo, 2016; Zinchenko et al., 2019). The main difference with those studies is that here we only focus on nonlinear eddies. Notably, the cyclonic drift of both CEs and AEs resembles the middepth cyclonic gyre circulation of the Lofoten Basin estimated from Argo float profiles for the time period 2002–2009 (Figure 7 in Voet et al., 2010). The middepth (1,000–1,500 m) circulation shown in their figure is also confined to the western part of the Lofoten Basin. Our analysis using Argo float data over a longer time period (2002–2018) found the same mean circulation pattern

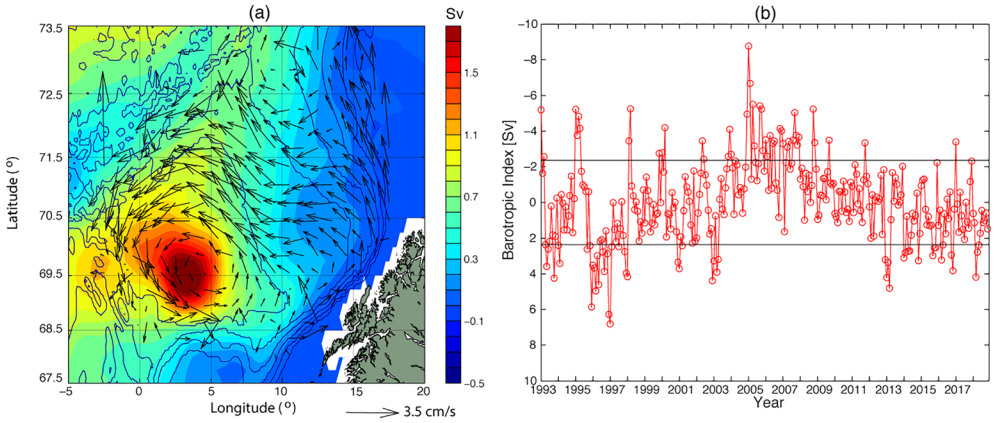

Figure 4. (a) EOF-1 of monthly barotropic stream function (TOPAZ reanalysis data), multiplied by the standard deviation of the corresponding principal component. Vectors superimposed on panel (a) show the mean drift velocity of nonlinear mesoscale eddies identified in this study. Blue isobaths are drawn for every 500 m. (b) Monthly deseasoned (1993–2018) time series of the gyre index. Black horizontal lines in panel (b) indicate the mean ±1 standard deviation.

(figure not shown), as shown by Voet et al. (2010). The similarity in the eddy drift pattern and the drift of Argo floats indicates a possible link between the cyclonic gyre circulation and the eddy drift.

The gyre circulation of the Lofoten Basin is investigated next using TOPAZ reanalysis data. Previous studies have successfully used TOPAZ data to study the gyre circulations in the Nordic Seas (Chatterjee et al., 2018; Raj et al., 2019). In here, Empirical orthogonal function (EOF) analysis is performed on the monthly barotropic stream function from TOPAZ reanalysis data to examine the spatial structure of the gyre circulation. Figure 4a presents the leading mode, explaining 35% of the variability, and features the known barotropic cyclonic circulation in the Lofoten Basin (e.g., Nøst & Isachsen, 2003). The figure shows the presence of the cyclonic gyre circulation in the reanalysis data, also confined to the western Lofoten Basin and thus matches the eddy drift pattern obtained from the altimeter data. Note that the velocity vector pointing northward in Figure 4a (at location 71.4°N and 2.5°W) is located in a grid where there are comparatively low number of eddy observations and may be an artifact. We use the area-averaged barotropic stream function over the western Lofoten Basin (bounded by 3,000-m isobaths in the region 2°W to 12°E and 68.5°N to 72°N; depth contour indicated in Figure 4a) as an indicator of the strength of the gyre circulation (Figure 4b; negative values indicate stronger cyclonic circulation); for simplicity we call it the "gyre index" hereafter. Note that we use actual values of the stream function to find the intensity/strength of the gyre instead of the gradient of stream function.

3.4. Interaction Between Mesoscale Eddies and the Gyre Circulation

The interaction between the gyre circulation and mesoscale eddies is investigated using composites maps of the eddy drift and EI of eddies during positive and negative gyre index (Figure 5). The positive/negative index are those months (deseasoned) with gyre index above/below mean ±1 standard deviation calculated over the entire period, 1993–2018. Note that while a negative gyre index represents stronger cyclonic circulation, positive gyre index represents a weakened cyclonic circulation. Figure 5 shows that the cyclonic drift of eddies is well defined during negative gyre index, that is, during strong cyclonic gyre circulation (Figure 5a). Similarly, a weakening of the gyre circulation is reflected as a less prominent signature of the cyclonic eddy drift (Figure 5b). However, there is no significant change in the mean drift speed of eddies during the two scenarios (4.8 and 4.6 cm/s).

On the other hand, the main change is found in the mean EI of eddies, which is higher/lower during negative/positive gyre index. The difference between the high (106 cm^2/s^2) and low (87 cm^2/s^2) EI is found to be statistically significant. Higher EI in the western Lofoten Basin during negative gyre index indicates the presence of a stronger Lofoten Vortex during the time period when the gyre is also strengthened. Interestingly, the EI in the eastern Lofoten Basin is also higher during a strengthened gyre, which points to the possible impact of a common forcing mechanism, and the impact of winds is a probable candidate.

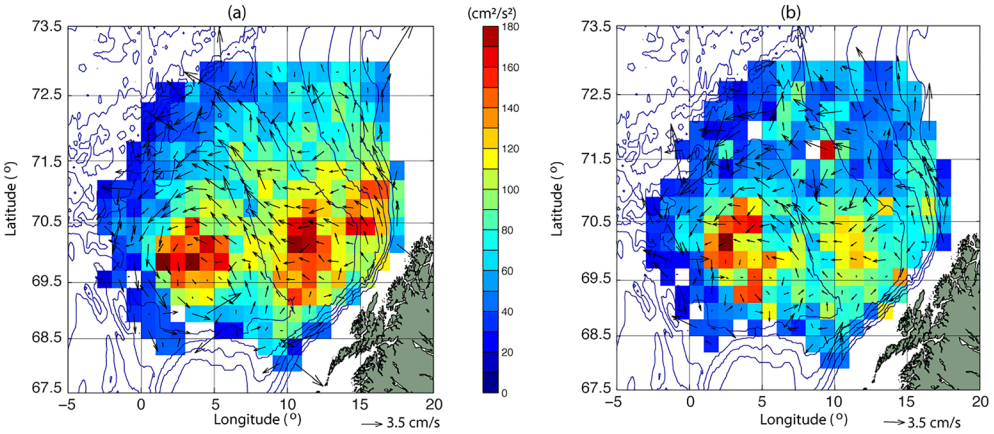

Figure 5. Mean (bin average) EI (color) and drift velocity (vectors) of eddies in the Lofoten Basin during (a) negative and (b) positive gyre index. Blue isobaths are drawn for every 500 m.

In a recent study, Raj et al. (2019) showed the impact of winds on the gyre index, which further supports the findings of previous studies reporting the influence of winds on the gyre circulation of the basin, via the barotropic response of the ocean to the overlying wind stress curl (e.g., Isachsen et al., 2003; Voet et al., 2010). The peak in the gyre index during early 2005 (Figure 4b) is associated with a low-pressure anomaly residing over the central Nordic Seas (figure not shown). At the same time winds are also known to influence mesoscale eddies of the eastern Lofoten Basin, via its impact on the slope current (Raj et al., 2018), thereby increasing the instability of the current and thus resulting in the shedding of energetic eddies (Raj et al., 2015).

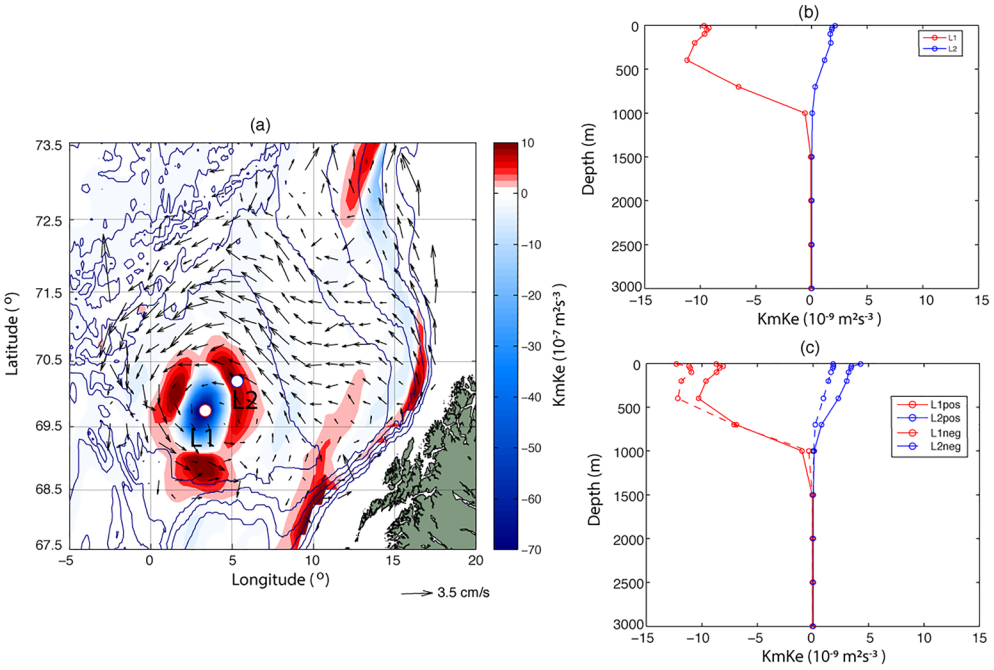

Figure 6. (a) Climatology (1993–2018) of barotopic energy conversion rate (KmKe; color) in the Lofoten Basin. Vectors superimposed on panel (a) show the mean drift velocity of nonlinear mesoscale eddies identified in this study. (b) Vertical profiles of KmKe at locations L1 and L2 (locations shown in panel a). Positive values indicate energy flow from mean flow to eddies, while negative values indicate the opposite flow. (c) Vertical profiles of KmKe at locations L1 (red) and L2 (blue) during negative (dashed) and positive (bold) gyre index.

Having established the coherence between EI and the gyre circulation, we further investigate the energy transfer between the mean flow and the eddies (Figure 6). Positive KmKe is an indicator of kinetic energy transfer from the mean flow to eddies. On the contrary, negative KmKe suggests energy transfer to the mean flow. Figure 6a shows KmKe integrated over the upper 1,000 m. In the deepest part of the basin (location of the Lofoten Vortex), KmKe is highly negative which indicates that the Lofoten Vortex can be a main source of energy for the mean flow. Interestingly, the Lofoten Vortex is surrounded by a region with positive KmKe, where the presence of CEs has been reported. The positive value implies the extraction of kinetic energy from the mean flow to eddies in these regions. The occurrence of shear instability in the barotropic slope current to the eddies resulting in the formation of mesoscale eddies, well documented in previous studies (e.g., Isachsen et al., 2012) is also represented in the figure.

The vertical profiles of KmKe at two different locations provide a detailed picture of the energy transfer from the mean to eddy fields and vice versa (Figure 6b). In the entire basin, the location of the Lofoten Vortex (L1) corresponds to the location with the peak energy transfer. The energy transfer from the eddy to the mean flow is even found at depths over 1,000 m. On the contrary location L2 represents the region where there is a considerable transfer of energy from the mean flow to eddies. However, in comparison the energy transfer at L2 is much smaller than at L1. KmKe averaged over 1,000-m depth at L2 is 0.7×10^{-9} m^2 s^{-3}, which is roughly 9 times smaller than that at L1 (6.4×10^{-9} m^2 s^{-3}). Composite profiles of KmKe for negative/positive gyre index are shown in Figure 6c. Notably, a higher/lower transfer of energy to the mean flow is found in the Lofoten Vortex region (L1) during negative/positive gyre index. That is, there is a larger transfer of energy from the Lofoten Vortex during the time period when the gyre is strengthened, in comparison to when it is weakened. This result is in line with the hypothesis of Voet et al. (2010) who argued that the eddies in the Lofoten Basin may influence the gyre circulation of the basin. On the other hand, at L2, a lower/higher transfer of energy from the mean flow to eddies is found during negative/positive gyre index. This indicates that there is less transfer of energy from the mean flow to the eddies during the time period when the gyre is strengthened; that is, less energy is spent on eddies. Hence, it can be summarized that the gyre circulation when strengthened, receives more energy from the Lofoten Vortex and loses less energy to those eddies circulating around the Lofoten Vortex, thereby acting as the shield to the vortex. We hypothesize that this balance in the transfer of energy between mesoscale eddies and the gyre circulation of the Lofoten Basin, in addition to the wind forcing, controls the strength of the gyre.

Our study thus provides the first evidence of the two-way interaction between the mesoscale eddies and the gyre circulation of the Lofoten Basin. Our study also confirms Voet et al.'s (2010) hypothesis that in addition to the effect of the wind forcing, mesoscale eddies of the Lofoten Basin also affects the gyre circulation basin. A more detailed study is recommended in order to understand the implications of this two-way interaction on the local eddy generation and on the water mass distribution inside the basin. A starting point can be to investigate (time series analysis/correlation analysis) the variability of the model-derived AW temperature in the Lofoten Basin during the altimeter era in relation to the variability of altimeter-derived eddy kinetic energy and model-derived KmKe.

4. Summary

The interaction between the gyre circulation and the mesoscale eddies in the Lofoten Basin is studied for the first time. Analysis used a suite of satellite altimeters, TOPAZ reanalysis and Argo floats for the purpose. Mesoscale eddies are identified using an automated hybrid eddy detection method which uses both geometrical and dynamical properties of the eddy for its detection. Argo floats profiles show that the eddy detection method used on altimeter data is able to successfully detect and differentiate anticyclonic and cyclonic eddies of the basin. A total of 5,373/5,589 individual anticyclonic/cyclonic eddies in the Lofoten Basin are detected from more than 65,000 altimeter-based eddy observations. The nonlinearity parameter is used to distinguish nonlinear eddies from linear wave disturbances. About 70–85% of the total eddies identified are found to be nonlinear. The analysis found clustering of nonlinear eddies on either side of the basin and the high eddy intensity associated with it. While high number of Eobs and EI of AEs on the eastern part is associated with the eddy generation from the slope current, the same in the western Lofoten Basin is linked to the near-permanent presence of the highly energetic Lofoten Vortex. CEs near the Lofoten

Vortex successfully resisting the tensile effect of the flow of the large vortex survive as localized vortex formations thereby add to high Eobs and EI of CEs in the western Lofoten Basin.

Further, we show the distinct cyclonic pattern of the drift of anticyclonic and cyclonic eddies in the Lofoten Basin, which is confined to the western side of the basin. The pattern of cyclonic middepth gyre circulation, also observed to be confined within the western Lofoten Basin, resembles that of the eddy drift. A well-defined cyclonic drift of eddies is found when the gyre circulation strengthens, while, when the gyre weakens, the cyclonic pattern of eddy drift is less pronounced. A detailed examination of the energy transfer is done by analyzing the barotropic energy conversion in the reanalysis data. The results show the maximum transfer of energy from the eddy field to the mean flow in the vicinity of the Lofoten Vortex. A smaller energy flux from the mean flow to eddies is observed outside the region of the Lofoten Vortex. Our results show that the Lofoten Vortex transfers more energy to mean flow when the gyre circulation strengthens. On the other hand, the gyre circulation transfers less energy to the eddies circulating around the Lofoten Vortex. In summary, we have shown that in addition to the wind forcing, the energy exchange between mesoscale eddies and the gyre circulation of the Lofoten Basin controls the strength of the gyre.

Data Availability Statement

Argo float data were collected and made freely available by the International Argo Program and the national programs that contribute to it (http://www.argo.ucsd.edu, http://argo.jcommops.org). The Argo Program is part of the Global Ocean Observing System. Argo float data collection (version 2.0; open access) organized according to ocean basins, for example, all Argo float profiles in the Atlantic Ocean can be obtained freely from ftp://ftp.ifremer.fr/ifremer/argo/geo/. The satellite altimeter data (product identifier: SEALEVEL_GLO_PHY_L4_REP_OBSERVATIONS_088_047) is freely made available by the Copernicus Marine Environmental Monitoring Service (ftp://my.cmems-du.eu/Core/SEALEVEL_GLO_PHY_L4_REP_OBSERVATIONS_008_047/dataset-duacs-rep-global-merged-allsat-phy-l4). The TOPAZ model data (product identifier: ARCTIC_REANALYSIS_PHYS_002_003) is also freely made available by CMEMS (ftp://my.cmems-du.eu/Core/ARCTIC_REANALYSIS_PHYS_002_003/dataset-ran-arc-myoceanv2-be). User registration is needed to download the data from CMEMS. Our study uses the latest version (Version 2) of the eddy detection and tracking algorithm detailed in Halo et al. (2014) and is made freely available at this site (http://doi.org/10.5281/zenodo.3862545).

Acknowledgments
This research is funded by the Copernicus Arctic MFC services (Grant 69). We also acknowledge the CPU provided by the Norwegian supercomputing project Sigma2 (nn2993k) and the storage space (ns2993k). Author S. Chatterjee thanks Nansen Scientific Society for the support provided. T. Belonenko, I. Bashmachnikov, and A. Fedorov acknowledge the Russian Science Foundation, project 18-17-00027.

References

Andersson, M., Orvik, K. A., Lacasce, J. H., Koszalka, I., & Mauritzen, C. (2011). Variability of the Norwegian Atlantic current and associated eddy field from surface drifters. *Journal of Geophysical Research: Oceans*, *116*, C08032. https://doi.org/10.1029/2011JC007078

Årthun, M., Eldevik, T., Smedsrud, L. H., Skagseth, Ø., & Ingvaldsen, R. B. (2012). Quantifying the influence of Atlantic heat on Barents Sea ice variability and retreat. *Journal of Climate*, *25*, 4736–4743. https://doi.org/10.1175/JCLI-D-11-00466.1

Bashmachnikov, I. L., Sokolovskiy, M. A., Belonenko, T. V., Volkov, D. L., Isachsen, P. E., & Carton, X. (2017). On the vertical structure and stability of the Lofoten vortex in the Norwegian Sea. *Deep-Sea Research Part I: Oceanographic Research Papers*, *128*, 1–27. https://doi.org/10.1016/j.dsr.2017.08.001

Belonenko, T. V., Volkov, D. L., Norden, Y. E., & Ozhigin, V. K. (2014). Circulation of waters in the Lofoten Basin of the Norwegian Sea. *Vestnik of St. Petersburg State University*, *7*(2), 108–121. (In Rusian)

Blindheim, J., & Rey, F. (2004). Water-mass formation and distribution in the Nordic Seas during the 1990s. *ICES Journal of Marine Science*, *61*(5), 846–863. https://doi.org/10.1016/j.icesjms.2004.05.003

Bloshkina, E. V., & Ivanov, V. V. (2016). Convective structures in the Norwegian and Greenland Seas according to results of modeling with a high spatial resolution. In *Works of Hydrometeorological Research Center of the Russian Federation*.

Capet, A., Mason, E., Rossi, V., Troupin, C., Faugère, Y., Pujol, I., & Pascual, A. (2014). Implications of refined altimetry on estimates of mesoscale activity and eddy-driven offshore transport in the eastern boundary upwelling systems. *Geophysical Research Letters*, *41*, 7602–7610. https://doi.org/10.1002/2014GL061770

Carton, X. J. (1992). On the merger of shielded vortices. *EPL*, *18*(8), 697–703. https://doi.org/10.1209/0295-5075/18/8/006

Chatterjee, S., Raj, R. P., Bertino, L., Skagseth, R., & Johannessen, O. M. (2018). Role of Greenland Sea gyre circulation on Atlantic water temperature variability in the Fram Strait. *Geophysical Research Letters*, *45*, 8399–8406. https://doi.org/10.1029/2018GL079174

Chelton, D. B., Schlax, M. G., & Samelson, R. M. (2011). Global observations of nonlinear mesoscale eddies. *Progress in Oceanography*, *91*(2), 167–216. https://doi.org/10.1016/j.pocean.2011.01.002

Chelton, D. B., Schlax, M. G., Samelson, R. M., & de Szoeke, R. A. (2007). Global observations of large oceanic eddies. *Geophysical Research Letters*, *34*, L15606. https://doi.org/10.1029/2007GL030812

Cronin, M., & Watts, D. R. (1996). Eddy-mean flow interaction in the Gulf Stream at 68°W. Part I: Eddy energetics. *Journal of Physical Oceanography*, *26*, 2107–2131. https://doi.org/10.1175/1520-0485(1996)026<2107:EFIITG>2.0.CO;2

Dong, C., McWilliams, J. C., & Shchepetkin, A. F. (2007). Island wakes in deep water. *Journal of Physical Oceanography*, *37*, 962–981. https://doi.org/10.1175/JPO3047.1

Dritschel, D. G. (1989). On the stabilization of a two-dimensional vortex strip by adverse shear. *Journal of Fluid Mechanics*, *206*, 193–221. https://doi.org/10.1017/S0022112089002284

Duacs/AVISO+ (2019). Mesoscale eddy trajectory Atlas product handbook, SALP-MU-P-EA-23126-CLS
Early, J. J., Samelson, R. M., & Chelton, D. B. (2011). The evolution and propagation of quasigeostrophic ocean eddies. *Journal of Physical Oceanography*, *41*, 1535–1555. https://doi.org/10.1175/2011JPO4601.1
Faghmous, J. H., Frenger, I., Yao, Y., Warmka, R., Lindell, A., & Kumar, V. (2015). A daily global mesoscale ocean eddy dataset from satellite altimetry. *Scientific Data*, *2*, 150,028. https://doi.org/10.1038/sdata.2015.28
Fedorov, A. M., Bashmachnikov, I. L., & Belonenko, T. V. (2019). Winter convection in the Lofoten Basin according to ARGO buoys and hydrodynamic modeling. *Vestnik of Saint Petersburg University. Earth Sciences*. https://doi.org/10.21638/spbu07.2019.308
Fedorov, A. M., & Belonenko, T. V. (2020). Interaction of Mesoscale vortices in the Lofoten Basin based on the GLORYS database. *Russian Journal of Earth Sciences*, *20*(2), ES2002. https://doi.org/10.2205/2020ES000694
Gascard, J. C., & Mork, K. A. (2008). Climatic importance of large-scale and mesoscale circulation in the Lofoten basin deduced from Lagrangian observations. In *Arctic-Subarctic ocean fluxes: Defining the role of the Northern Seas in climate*. https://doi.org/10.1007/978-1-4020-6774-7_7
Halo, I. (2012). The Mozambique Channel eddies: Characteristics and mechanisms of formation (Ph.D. thesis). University of Cape Town. http://hdl.handle.net/11427/6477
Halo, I., Backeberg, B., Penven, P., Ansorge, I., Reason, C., & Ullgren, J. E. (2014). Eddy properties in the Mozambique Channel: A comparison between observations and two numerical ocean circulation models. *Deep-Sea Research Part II: Topical Studies in Oceanography*, *100*, 38–53. https://doi.org/10.1016/j.dsr2.2013.10.015
Helland-Hansen, B., & Nansen, F. (1909). The Norwegian Sea: Its physical oceanography based upon the Norwegian research 1900-1904. In *Report on Norwegian Fishery and Marine Investigations* (Vol. *2*).
Isachsen, P. E., Koszalka, I., & Lacasce, J. H. (2012). Observed and modeled surface eddy heat fluxes in the eastern Nordic Seas. *Journal of Geophysical Research: Oceans*, *117*, C08020. https://doi.org/10.1029/2012JC007935
Isachsen, P. E., LaCasce, J. H., Mauritzen, C., & Häkkinen, S. (2003). Wind-driven variability of the large-scale recirculating flow in the Nordic Seas and Arctic Ocean. *Journal of Physical Oceanography*, *33*, 2534–2550. https://doi.org/10.1175/1520-0485(2003)033<2534:WVOTLR>2.0.CO;2
Isachsen, P. E. (2015). Baroclinic instability and the mesoscale eddy field around the Lofoten Basin. *Journal of Geophysical Research: Oceans*, *120*, 2884–2903. https://doi.org/10.1002/2014JC010448
Isachsen, P. E., Mauritzen, C., & Svendsen, H. (2007). Dense water formation in the Nordic Seas diagnosed from sea surface buoyancy fluxes. *Deep-Sea Research Part I: Oceanographic Research Papers*, *54*(1), 22–41. https://doi.org/10.1016/j.dsr.2006.09.008
Isern-Fontanet, J., García-Ladona, E., & Font, J. (2006). Vortices of the Mediterranean Sea: An altimetric perspective. *Journal of Physical Oceanography*, *36*, 87–103. https://doi.org/10.1175/JPO2826.1
Jakobsen, P. K., Ribergaard, M. H., Quadfasel, D., Schmith, T., & Hughes, C. W. (2003). Near-surface circulation in the northern North Atlantic as inferred from Lagrangian drifters: Variability from the mesoscale to interannual. *Journal of Geophysical Research C: Oceans*, *108*, 3251. https://doi.org/10.1029/2002jc001554
Klein, P., Hua, B. L., Lapeyre, G., Capet, X., Le Gentil, S., & Sasaki, H. (2008). Upper ocean turbulence from high-resolution 3D simulations. *Journal of Physical Oceanography*, *38*, 1748–1763. https://doi.org/10.1175/2007JPO3773.1
Köhl, A. (2007). Generation and stability of a quasi-permanent vortex in the Lofoten Basin. *Journal of Physical Oceanography*, *37*, 2637–2651. https://doi.org/10.1175/2007JPO3694.1
Kundu, P. K. (1990). *Fluid mechanics* (Vol. 1, p. 638). San Diego, CA: Academic.
Le Traon, P. Y., & Ogor, F. (1998). ERS-1/2 orbit improvement using TOPEX/POSEIDON: The 2 cm challenge. *Journal of Geophysical Research*, *103*(C4), 8045–8057. https://doi.org/10.1029/97jc01917
Lien, V. S., Hjøllo, S. S., Skogen, M. D., Svendsen, E., Wehde, H., Bertino, L., et al. (2016). An assessment of the added value from data assimilation on modelled Nordic seas hydrography and ocean transports. *Ocean Modelling*, *99*, 43–59. https://doi.org/10.1016/j.ocemod.2015.12.010
Marchesiello, P., McWilliams, J. C., & Shchepetkin, A. (2003). Equilibrium structure and dynamics of the California current system. *Journal of Physical Oceanography*, *33*, 753–783. https://doi.org/10.1175/1520-0485(2003)33<753:ESADOT>2.0.CO;2
McWilliams, J. C., & Flierl, G. R. (1979). On the evolution of isolated, nonlinear vortices. *Journal of Physical Oceanography*, *9*, 1155–1182. https://doi.org/10.1175/1520-0485(1979)009<1155:oteoin>2.0.co;2
Mizobata, K., Saitoh, S. I., Shiomoto, A., Miyamura, T., Shiga, N., Imai, K., et al. (2002). Bering Sea cyclonic and anticyclonic eddies observed during summer 2000 and 2001. *Progress in Oceanography*, *55*(55), 65–75. https://doi.org/10.1016/S0079-6611(02)00070-8
Mohn, H. (1887). The Northern Ocean, its depths, temperature and circulation. In *The Norwegian North-Atlantic Expedition 1876–1878* (Vol. 2, pp. (1–209). Christiania (in Norwegian): Grøndahl and Son.
Nøst, O. A., & Isachsen, P. E. (2003). The large-scale time-mean ocean circulation in the Nordic Seas and Arctic Ocean estimated from simplified dynamics. *Journal of Marine Research*, *61*, 175–210. https://doi.org/10.1357/002224003322005069
Orvik, K. A. (2004). The deepening of the Atlantic water in the Lofoten Basin of the Norwegian Sea, demonstrated by using an active reduced gravity model. *Geophysical Research Letters*, *31*, L01306. https://doi.org/10.1029/2003GL018687
Orvik, K. A., & Niiler, P. (2002). Major pathways of Atlantic water in the northern North Atlantic and Nordic Seas toward Arctic. *Geophysical Research Letters*, *29*(19), 1896. https://doi.org/10.1029/2002GL015002
Orvik, K. A., & Skagseth, Ø. (2003). Monitoring the Norwegian Atlantic slope current using a single moored current meter. *Continental Shelf Research,* Volume *23*, Issue 2, 159–176, https://doi.org/10.1016/S0278-4343(02)00172-3
Penven, P., Echevin, V., Pasapera, J., Colas, F., & Tam, J. (2005). Average circulation, seasonal cycle, and mesoscale dynamics of the Peru current system: A modeling approach. *Journal of Geophysical Research*, *110*, C10021. https://doi.org/10.1029/2005JC002945
Poulain, P. M., Warn-Varnas, A., & Niiler, P. P. (1996). Near-surface circulation of the Nordic seas as measured by Lagrangian drifters. *Journal of Geophysical Research*, *101*(C8), 18,237–18,258. https://doi.org/10.1029/96JC00506
Raj, R. P., Chatterjee, S., Bertino, L., Turiel, A., & Portabella, M. (2019). The Arctic front and its variability in the Norwegian Sea. *Ocean Science*, *15*, 1729–1744. https://doi.org/10.5194/os-15-1729-2019
Raj, R. P., Johannessen, J. A., Eldevik, T., Nilsen, J. E. Ø., & Halo, I. (2016). Quantifying mesoscale eddies in the Lofoten Basin. *Journal of Geophysical Research: Oceans*, *121*, 4503–4521. https://doi.org/10.1002/2016JC011637
Raj, R. P., Chafik, L., Nilsen, J. E. Ø., Eldevik, T., & Halo, I. (2015). The Lofoten vortex of the Nordic seas. *Deep-Sea Research Part I: Oceanographic Research Papers*, *96*, 1–14. https://doi.org/10.1016/j.dsr.2014.10.011
Raj, R. P., & Halo, I. (2016). Monitoring the mesoscale eddies of the Lofoten Basin: Importance, progress, and challenges. *International Journal of Remote Sensing*, *37*, 163,712–163,728. https://doi.org/10.1080/01431161.2016.1201234

Raj, R. P., Nilsen, J. E. Ø., Johannessen, J. A., Furevik, T., Andersen, O. B., & Bertino, L. (2018). Quantifying Atlantic water transport to the Nordic Seas by remote sensing. *Remote Sensing of Environment*, *216*, 758–769. https://doi.org/10.1016/j.rse.2018.04.055

Rossby, T., Prater, M. D., & Søiland, H. (2009). Pathways of inflow and dispersion of warm waters in the Nordic seas. *Journal of Geophysical Research*, *114*, C04011. https://doi.org/10.1029/2008JC005073

Sandø, A. B., Nilsen, J. E. Ø., Gao, Y., & Lohmann, K. (2010). Importance of heat transport and local air-sea heat fluxes for Barents Sea climate variability. *Journal of Geophysical Research*, *115*, C07013. https://doi.org/10.1029/2009JC005884

Segtnan, O. H., Furevik, T., & Jenkins, A. D. (2011). Heat and freshwater budgets of the Nordic Seas computed from atmospheric reanalysis and ocean observations. *Journal of Geophysical Research*, *116*, C11003. https://doi.org/10.1029/2011JC006939

Skagseth, Ø., & Orvik, K. A. (2002). Identifying fluctuations in the Norwegian Atlantic slope current by means of empirical orthogonal functions. *Continental Shelf Research*, *22*(4), 547–563. https://doi.org/10.1016/S0278-4343(01)00086-3

Snedecor, G. W., & Cochran, W. G. (1989). *Statistical methods* (8th ed.). Ames, IA: Iowa State Univ. Press.

Theiss, J. (2004). Equatorward energy cascade, critical latitude, and the predominance of cyclonic vortices in geostraphic turbulence. *Journal of Physical Oceanography*, *34*, 1663–1678. https://doi.org/10.1175/1520-0485(2004)034<1663:EECCLA>2.0.CO;2

Tóth, G., & Házi, G. (2010). Merging of shielded Gaussian vortices and formation of a tripole at low Reynolds numbers. *Physics of Fluids*, *22*, 053101. https://doi.org/10.1063/1.3428539

Travkin, V. S., & Belonenko, T. V. (2019). Seasonal variability of mesoscale eddies of the Lofoten Basin using satellite and model data. *Russian Journal of Earth Sciences*, *19*(5), ES5004. https://doi.org/10.2205/2019ES000676

Tulloch, R., Marshall, J., & Smith, K. S. (2009). Interpretation of the propagation of surface altimetric observations in terms of planetary waves and geostrophic turbulence. *Journal of Geophysical Research*, *114*, C02005. https://doi.org/10.1029/2008JC005055

Voet, G., Quadfasel, D., Mork, K. A., & Søiland, H. (2010). The mid-depth circulation of the Nordic Seas derived from profiling float observations. *Tellus. Series A: Dynamic Meteorology and Oceanography*, *62*(4), 516–529. https://doi.org/10.1111/j.1600-0870.2010.00444.x

Volkov, D. L., Belonenko, T. V., & Foux, V. R. (2013). Puzzling over the dynamics of the Lofoten Basin—A sub-Arctic hot spot of ocean variability. *Geophysical Research Letters*, *40*, 738–743. https://doi.org/10.1002/grl.50126

Volkov, D. L., Kubryakov, A. A., & Lumpkin, R. (2015). Formation and variability of the Lofoten basin vortex in a high-resolution ocean model. *Deep-Sea Research Part I: Oceanographic Research Papers*, *105*, 142–157. https://doi.org/10.1016/j.dsr.2015.09.001

Walczowski, W., & Piechura, J. (2011). Influence of the West Spitsbergen current on the local climate. *International Journal of Climatology*, *31*, 1088–1093. https://doi.org/10.1002/joc.2338

Wunsch, C. (2010). Toward a midlatitude ocean frequency-wavenumber spectral density and trend determination. *Journal of Physical Oceanography*, *40*, 2264–2281. https://doi.org/10.1175/2010JPO4376.1

Xie, J., Bertino, L., Knut, L., & Sakov, P. (2017). Quality assessment of the TOPAZ4 reanalysis in the Arctic over the period 1991–2013. *Ocean Science*, *13*, 123–144. https://doi.org/10.5194/os-13-123-2017

Xie, J., Sakov, P., Counillon, F., Bertino, L., Raj. R. P., & Lien, V. S. (2020). *Quality information document for Arctic physical reanalysis product*, ARCTIC_REANALYSIS_PHY_002_003. Retrieved from http://resources.marine.copernicus.eu/documents/QUID/CMEMS-ARC-QUID-002-003.pdf

Yu, L. S., Bosse, A., Fer, I., Orvik, K. A., Bruvik, E. M., Hessevik, I., & Kvalsund, K. (2017). The Lofoten Basin eddy: Three years of evolution as observed by Seagliders. *Journal of Geophysical Research: Oceans*, *122*, 6814–6834. https://doi.org/10.1002/2017JC012982

Zinchenko, V. A., Gordeeva, S. M., Sobko, Y. V., & Belonenko, T. V. (2019). Analysis of Mesoscale eddies in the Lofoten Basin based on satellite altimetry. *Fundamental'anja i prikladnaja gidrofizika (Fundamental and Applied Hydrophysics).*, *12*(3), 46–54. https://doi.org/10.7868/S2073667319030067